VOLUME 35 NUMBER 3

ACCOUNTS of CHEMICAL RESEARCH®

MARCH 2002

A View at the Millennium: the Efficiency of Enzymatic Catalysis

THOMAS C. BRUICE

Department of Chemistry and Biochemistry, University of California, Santa Barbara, California 93106

Received March 8, 2001

ABSTRACT

Binding TS in preference to S and increasing $T\Delta S^{\ddagger}$ by freezing out motions in E·S and E·TS have been accepted as the driving forces in enzymatic catalysis; however, the smaller value of $\Delta G^{\ddagger}$ for a one-substrate enzymatic reaction, as compared to its nonenzymatic counterpart, is generally the result of a smaller value of $\Delta H^{\ddagger}$. Ground-state conformers (E·NACs) are formed in enzymatic reactions that structurally resemble E·TS. E·NACs are in thermal equilibrium with all other E·S conformers and are turnstiles through which substrate molecules must pass to arrive at the lowest-energy TS. TS in E·TS may or may not be bound tighter than NAC in E·NAC.

1. Introduction

Pauling proposed[1,2] in 1946 that the active site of an enzyme binds the transition state (TS) in preference to the substrate (S) and by doing so, stabilizes the TS and lowers the activation energy (Chart 1). This proposal has had great popular acceptance[3,4]

Shortly after the first bimolecular-nucleophilic catalysis of ester hydrolysis by organic bases was reported (1956–57),[5–7] studies showing the effectiveness of intramolecular-nucleophilic catalysis of the hydrolysis of acetals, esters, amides, and imine bases were published.[8,9] Studies of intramolecular-nucleophilic catalysis continue.[10,11] On the basis of kinetic data for the intramolecular-nucleophilic-catalyzed hydrolysis of a series of dicarboxylic acid monoesters (Table 1), Bruice and Pandit proposed[12] that

Chart 1

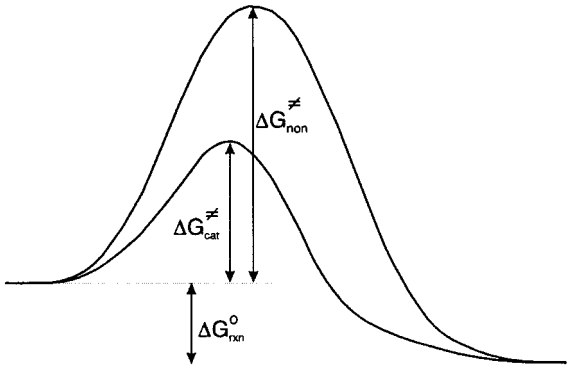

one-substrate enzymatic reactions could exhibit rate enhancements of 10^8-fold, as compared to a corresponding bimolecular reaction, if the substrate were held in a conformation that closely resembled the transition state.

Page and Jencks[13] provided another explanation for the data of Table 1. They reasoned that translational and rotational freedom of motion of reactants in a bimolecular reaction would be frozen out on conversion to an effective intramolecular reaction or a one-substrate enzymatic reaction. Using standard formulas for the partition function and estimated moments of inertia, they approximated the entropy for two nonpolar molecules undergoing a pericyclic reaction in water. The difference in the $\Delta G^{\ddagger}$ of reaction, when corrected for entropic contributions of motion plus the dampening of vibrational low frequencies in the TS, was concluded to be sufficient to provide a 10^8-fold increase in rate. From this, it became common knowledge that a 10^8-fold increase in rate was to be expected in comparing a bimolecular reaction to a single-substrate enzymatic reaction.[13,14] This has been termed the "entropy trap". Computations employing the more desirable cratic entropy methods establish that the Sackur–Tetrode calculations of entropy by Page and Jencks are largely overestimated.[16b]

2. The Entropy Trap

The activation parameters for a series of one-substrate enzyme-catalyzed reactions (yeast OMP decarboxylase,

Thomas C. Bruice has been a member of the U.S. Navy amphibious forces (1943–1946) and the faculties of Yale, Johns Hopkins, and Cornell Universities and the University of California at Santa Barbara, where he is presently Research Professor. Bruice has published well over 500 scientific papers. The inventor of the term "bioorganic chemistry", he has contributed importantly to many areas of mechanistic chemistry dealing with the problems of interest in biochemisty. His accomplishments have been recognized by a number of prestigious awards.

10.1021/ar0001665 CCC: $22.00
Published on Web 01/18/2002

Table 1

$$CH_3CO_2^- + CH_3CO_2C_6H_4Br(p) \xrightarrow{k_{rel}=1.0\ M} (CH_3CO)_2O + {}^-OC_6H_4Br(p)$$

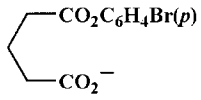

~ 1 x 10^3 M

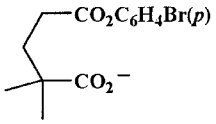

~ 3.6 x 10^3 M

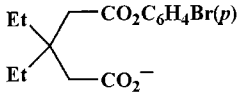

~ 1.8 x 10^5 M

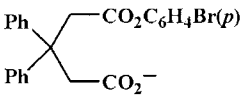

~ 2.7 x 10^5 M

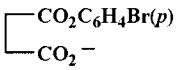

~ 2.3 x 10^5 M

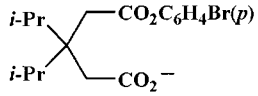

~ 1.3 x 10^6 M

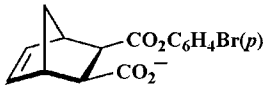

~ 8 x 10^7 M

urease, bacterial α-glucosidase, staphylococcal nuclease, chymotrypsin, and *Bacillus subtilis* chorismate mutase) have been compared to those for the corresponding nonenzymatic reactions.[15] It was found that average $T\Delta S^{\ddagger}$ values are similar for the enzymatic reactions (k_{cat}) and for their noncatalyzed counterparts (k_{non}). For these single-substrate enzymes, the large difference between $\Delta G^{\ddagger}_{enz}$ and $\Delta G^{\ddagger}_{non}$ arises from a difference in $\Delta H^{\ddagger}$. Similar observations have been made for antibody catalysts.[16a] It should be remembered that $\Delta H^{\ddagger}$ and $T\Delta S^{\ddagger}$ terms are often related (compensation effect), and this is so in many enzymtic reactions. Comparisons of activation parameters[17] for the pericyclic rearrangement of chorismate to prephenate (in water, $\Delta H^{\ddagger} = 20.5$ kcal/mol, $-T\Delta S^{\ddagger} = 3.9$ kcal/mol; with *B. subtilis* mutase, $\Delta H^{\ddagger} = 12.7$ kcal/mol, $-T\Delta S^{\ddagger} = 2.7$ kcal/mol; with *Escherichia coli* mutase, $\Delta H^{\ddagger} = 16.3$ kcal/mol, $-T\Delta S^{\ddagger} = 0.9$ kcal/mol) show that the values of $\Delta G^{\ddagger}$ for the two enzyme-catalyzed reactions are closely similar but the ratios of $(\Delta H^{\ddagger})/(-T\Delta S^{\ddagger})$ are quite different (5.25 vs 18). In comparing the reactions in water to the enzymatic reaction, the values of $\Delta\Delta G^{\ddagger}$ are dependent on the change in enthalpy for the *B. subtilis* enzyme and on both enthalpy and entropy for the *E. coli* enzyme. For enzymatic reactions involving more than one substrate, it is expected that the value of $T\Delta S^{\ddagger}$ would increase. This is so for a glutamate dehydrogenase reaction, the only two-substrate reaction for which activation parameters have been published.[18] It is well-known (by NMR[19]) that protein structures are in constant motion. One may observe the motions of the substrate and transition state in enzyme-catalyzed reactions by molecular dynamic (MD) simulations. There is a great deal of motion in both the substrate and the enzyme in the E·S complex. With the exception, perhaps, of the angle and partial bond length of the bond being made, there is also considerable motion along the reaction coordinate leading to E·TS formation. Thus, freezing out torsional motions in enzymatic reactions is far less important than envisioned by Page and Jencks. In addition, their assumption that freezing out frequencies lower than 1000 cm^{-1} in the transition state contributes to the decrease in activation energy required for rate enhancements of 10^8-fold has no basis. [20−22]

Warshel[22] offers a computer-simulation approach to determine the entropic contribution of the reactants to the free energy of enzymatic catalysis. The approach was designed to evaluate the difference between $\Delta S^{\ddagger}$ of an enzymatic reaction and the corresponding reference reaction in a solvent cage. It was concluded that many of the motions that are free in solution are also free in the transition state, and the binding of substrate to the enzyme does not completely freeze out the motion of the reacting fragments. The entropic contributions of the reacting fragments were computed to be "not so different in the enzyme and in the solvent cage".

3. Model Intramolecular Reactions and the Concept of Near-Attack Conformers (NACs)

Conformational analysis, using a combination of stochastic search[23] and molecular mechanics,[24] of the conformers of each ester in Table 1 was carried out.[25] The results of the study showed that the most stable conformers are extended (with the reacting $-CO_2^-$ and $-CO_2R$ groups as far apart as possible) and that the reactions take place through near-attack conformers (NACs) that clearly resemble the transition state. For reactions involving bonding between O, N, C, and S atoms, NACs are characterized as having reacting atoms within 3.2 Å and an approach angle for reaction of ±15° of the bonding angle in the transition state (Chart 2). A distance of 3.2 Å places the reacting atoms at a contact distance equal to about the sum of their van der Waals radii. The energy of the conformers does not change when the angle of approach deviates by ±15° from the bonding angle in the transition state for nucleophilic attack on sp^3 or sp^2 carbons sepa-

Chart 2

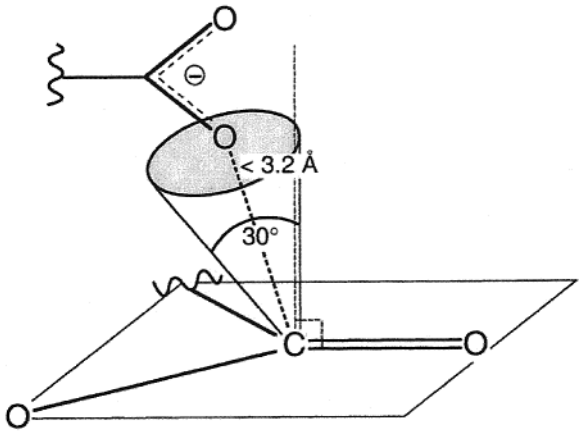

rated by 3.2 Å.[26] The mole fraction (P) of ground state conformers that are NACs was calculated for each ester from the energies of all conformers for each ester using a Boltzmann distribution. The relationship shown in eq 1 was

$$\log k_{rel} = 0.94 \log P + 7.48 \ (R^2 = 0.915) \qquad (1)$$

found (Figure 1). The value of P is determined by the preorganization of the ground-state structure and is reflected in $\Delta H°$ rather than in the phase−space entropy, $T\Delta S°$. Thus, the rate constants of Table 1 are directly dependent on the population of NACs for each ester.

4. Computational Methods for Enzymatic Reactions

Comparison of the dynamic structures of E·S and E·TS allows (i) the observation of ground-state NAC formation, (ii) the contrast in E·NAC and E·TS structures, and (iii) an evaluation of the importance of transition-state binding in comparison to the binding of ground-state NAC. If electrostatic, dipolar, and hydrophobic interactions are comparable in ground-state E·NAC and in E·TS, it can be concluded that the binding of TS and NAC by the enzyme is much the same. Experimental procedures have yet to be developed that directly measure the strengths of the interactions in E·TS. We have used molecular dynamic (MD) simulations starting with the X-ray coordinates of E·S (or E·I, which is convertible to E·S) and derived starting coordinates for TS to determine the dynamic structures of E·S and E·TS. The advantage of classical MD simulations is that relatively long time periods are available for structure sampling. A disadvantage is that neither the activation energy nor the free energies of activation ($\Delta G^{\ddagger}$) can be determined easily. A number of computational procedures[27,28] are used to determine activation energies or free energies of activation for E·S → E·TS starting with the X-ray-derived coordinates of E·S. In the QM/MM methodologies for the determination of activation energies, bond formation and bond breaking at the reactive site are described by quantum mechanics (QM), but a molecular mechanics (MM) computed empirical force field determines the structure of the remainder of the system. The use of ab initio or density functional methods suffers in that the QM portion of QM/MM can reasonably handle only about 40 atoms. Semiempirical (AM1, PM3) methods can handle hundreds of atoms, but may lack the needed accuracy. The use of semiempirical methods for the QM portion is acceptable, providing that it has been shown in a nonenzymatic model that the semiempirical procedure provides results similar to those from a higher-level computation for the reaction at hand. If not, the semiempirical parameters should be reparametrized,[29] or energy surfaces created by AM1 can be iterated by a higher-order QM. The QM-free energy (QM-FE) method involves the determination of the reaction path in vacuo employing a high-level QM procedure. This is followed by a series of QM/MD simulations at points

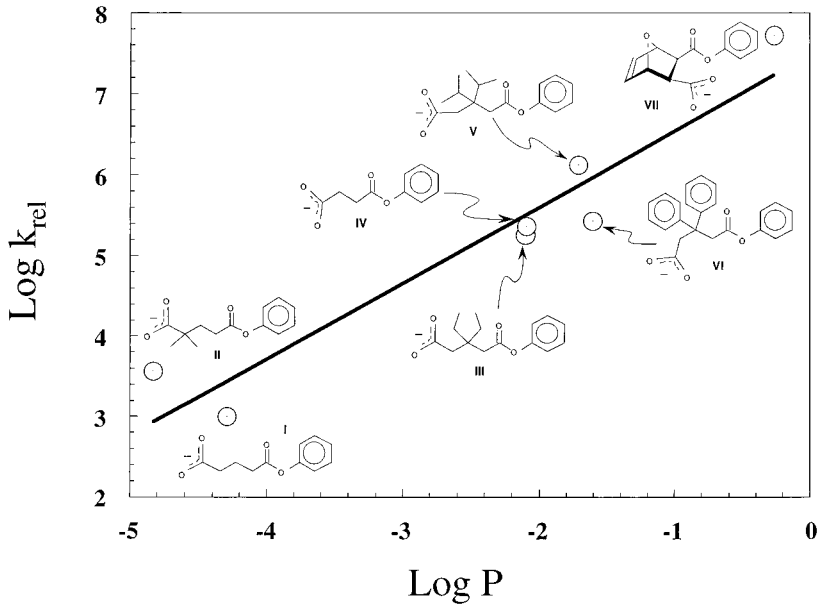

FIGURE 1. Plot of the log of the relative rate constants (k_{rel}) of Table 1 vs log of the probability (P) for NAC formation for each ester.

along the reaction path in the enzyme. The QM-FE procedure[28] has the advantage of using high-level QM calculations, but it suffers in that the gas-phase structures and their charges are not altered by being placed in the active site of the enzyme. The energies of the gas-phase structures are, however, influenced by the enzyme structure. QM/MM, even if supplemented by umbrella sampling, and QM-FE methods do not involve as extensive sampling of structural states as do classical MD simulations taken to the nanosecond time scale.

5. How Is the Value of K_{TS} Related to the Tightness of Binding of TS to the Active Site?

In Scheme 1, k_{non} and k_{cat}/K_M are the first-order and

Scheme 1

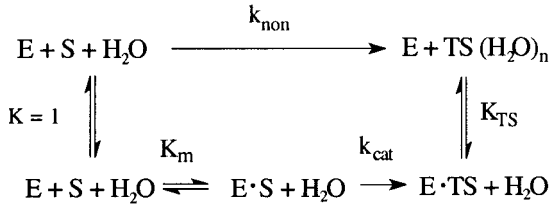

second-order rate constants for the spontaneous conversion of substrate to product in water and for the enzymatic reaction, respectively. According to transition-state theory, the ground states of both reactions are in equilibrium with their transition states. Since the ground states are identical (H_2O + enzyme + substrate), a thermodynamic cycle is created when the two transition states are placed in equilibrium (eq 2)

$$E{\cdot}TS + (H_2O)_n \overset{K_{TS}}{\rightleftharpoons} E + TS(H_2O)_n \qquad (2)$$

It has been concluded, accepting Scheme 1 and eq 2, that the binding affinity of E for TS exceeds the binding affinity of $(H_2O)_n$ for TS by a factor (K_{TS}) that matches the increase in rate that the catalyst produces. In other words, the efficiency of enzymatic reactions can be explained entirely by preferential enzyme binding of TS.[31] If K_{TS} is to be accepted as a measure of the difference in interaction energies of a TS with enzyme and with water (eq 2),[31] the transition states generated in water and in the enzymatic reaction should be identical. How often is this so?

There is an alternate explanation that satisfies eq 2 and the equilibrium between ground state and transition state that is required by transition state theory. The *stability* of a given TS is dependent upon its free energy content when compared to the ground state ($\Delta G^{\ddagger}_{enz}$ and $\Delta G^{\ddagger}_{non}$ in Scheme 2). The difference in stability of two transition states (E·TS and $TS(H_2O)_n$) sharing a common ground state is the difference in their free energy content (eq 3).

$$\Delta G^{o}_{KTS} = \Delta G^{\ddagger}_{enz} - \Delta G^{\ddagger}_{non} \qquad (3)$$

The standard free energy of the equilibrium of eq 2 (ΔG^{o}_{KTS}) is then determined by those features that determine the free energies of activation for the enzymatic and nonenzymatic reactions. Transition-state binding may or

Scheme 2

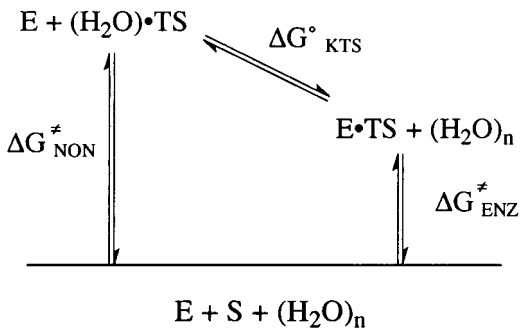

may not be one of those features. A computational comparison (QM-FE) of transition states in enzyme and in water by Peter Kollman[30] indicated that transition-state stabilization by the enzyme is too small to explain enzymatic rates.

Pauling's proposal[1,2] was that the efficiency of enzymatic reactions is dependent upon the preferential binding of the transition state compared to the ground state. We have chosen to employ ab initio and molecular dynamic procedures to compare the structures of E·S and E·TS as an approach to the question of preferential TS, as compared to S, binding in enzymatic reactions. The results so obtained are then compared to predictions from comparisons of the experimental value of $1/K_S$ for substrate binding and $1/K_{TS}$ ($= k_{cat}/K_M k_{non}$).

For our stated purpose, enzymatic reactions that involve formation and breakdown of covalent intermediates have been avoided, since the transition states are bonding (or bound) to the enzyme. Therefore, they cannot exist in equilibrium with the transition state in water (eq 2). For similar reasons, reactions involving the formation of covalent bonds between substrate and coenzyme have not been included. We have chosen to examine enzymatic reactions that involve only electrostatic, dipolar, and hydrophobic interactions between enzyme and S and TS.

It is understood that one can calculate a value of $K_{TS} = K_M(k_{non}/k_{cat})$ for *any enzymatic reaction*. K_{TS} is a measure of the relative activation free energies ($\Delta\Delta G^{\ddagger} = \Delta G_{non}^{\ddagger} - \Delta G_{enz}^{\ddagger}$) of any enzymatic and nonenzymatic reaction and all the features that go into the determination of the values of $\Delta G_{ENZ}^{\ddagger}$ and $\Delta G_{non}^{\ddagger}$.[32] From plots of log k_{non} vs $-\log K_{TS}$ and log k_{cat} vs $-\log K_{TS}$, one finds that log k_{non} decreases as $-\log K_{TS}$ increases [slope, -0.95; $R = 0.96$], but log k_{cat} is essentially independent of $-\log K_{TS}$.[31] Thus, the slower the nonenzymatic reaction, the greater must be the efficiency ($1/K_{TS}$) of the enzymatic reaction in order to achieve a k_{cat} essential for biological processes. This is a satisfying observation.

6. Examination of Several Enzymatic Reactions That Do Not Involve Covalent Intermediates

The chorismate mutase enzymes catalyze the Claisen rearrangement of chorismate to prephenate (Chart 3)[33,34] The catalysis involves *only* electrostatic and van der Waals interactions of the enzyme with both the substrate and transition state. Studies with the *B. subtilis* enzyme have

Chart 3

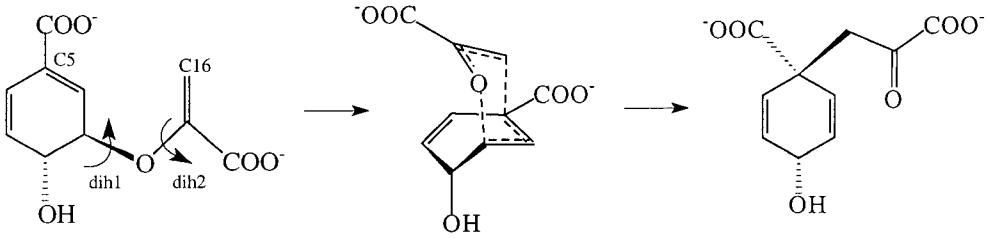

Chorismate Transition State Prephenate

Chart 4

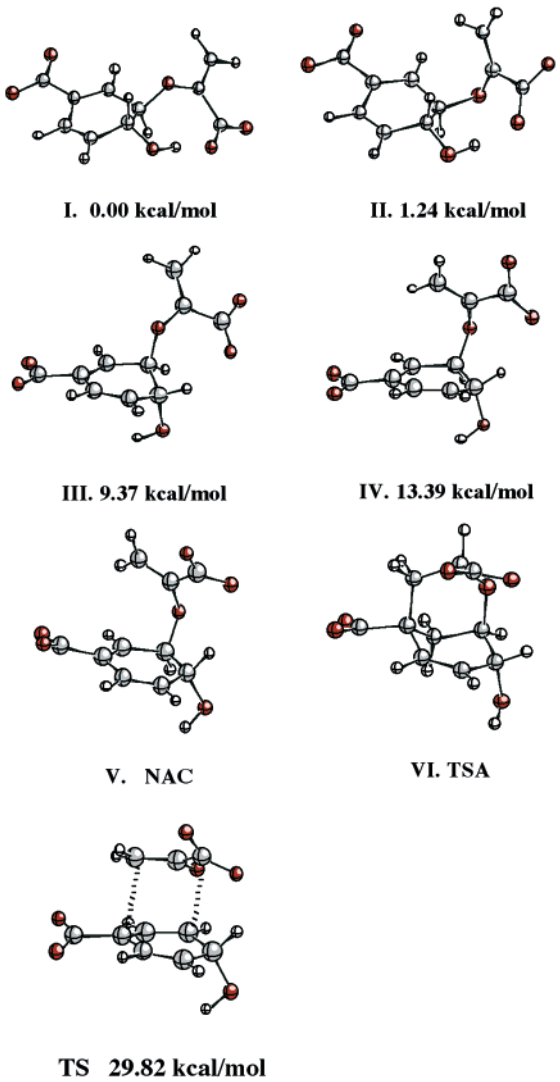

provided evidence in support of the enzyme's stabilizing a conformer capable of progressing into the transition state for prephenate product formation.[35,36] We have examined the *E. coli* chorismate mutase enzyme (EcCM). Chorismate exists in four principal conformations and the TS for chorismate → prephenate has been identified[37] by B3YLP/6-31+G(d,p) (Chart 4). The value of K_M/K_{TS} can be calculated to be 2×10^6. As we shall see, stabilization of the TS has nothing to do with the mechanism of EcCM.

We have examined the 2-ns MD simulations of EcCM with chorismate conformers **II** and **IV** initially docked at the active site. The binding of the abundant conformer **II** is followed by a kinetic step in which **II** is converted to an intermediate structure, which is then converted to a NAC. The NAC then goes onto the TS with little expenditure of energy. This sequence of events explains why secondary isotope effects are not observed. For convenience, most of the studies were initiated with both the most NAC-like conformer of chorismate (**IV**) and the TS docked at the active site.[37] The EcCM active site is extremely proficient in inducing the rearrangement of substrate (**II** and, particularly, **IV**) to form a NAC. The electrostatic and hydrophobic interactions between EcCM and chorismate are identified in Chart 5. The preorganization of the EcCM structure sturdily holds the guanidine substituents of Arg11* and Arg28 in place. The two carboxylate groups of the substrate are electrostatically bound to Arg11* and Arg28, which are separated by a distance that requires a change in structure of the chorismate conformers (**II** or **IV**) to a conformation in which the reactive C16 terminus is tucked under Val35. The enforced changes in conformation result from twisting around the two dihedral angles (dh1 and dh2 of Chart 3). The van der Waals contact of C16 with Val35 restricts the space between reactive termini (C16 and C5), resulting in a shorter C5−C16 distance. There is no strain on the substrate by the van der Waals contact with Val35. Seventy percent of chorismate exists in this "active site box" as NACs. When EcCM·NAC → EcCM·TS, there is no change in the various electrostatic interactions with Arg11*, Arg28, Gln88, and Lys39, but the lyophobic interactions of Arg51, Ile81, and Val35 are released. It is concluded that the $>10^6$ rate enhancement by the enzyme is overwhelmingly due to the conformational restriction of ground-state structures to NACs. Menger has shown in synthetic chorismate-like model systems that conformational restriction to a NAC-like conformer provides rate enhancements equal to that of the enzymatic reaction.[36]

The binding of transition-state analogues, such as **VI**, has been offered in support of TS stabilization's being the driving force in catalysis by EcCM. When comparing **VI** to the stable conformers of chorismate (**I**, **II**, **III**) and to the NAC and TS structures of **Chart 4**, it is seen that the two carboxylate groups of **VI** are positioned as in the NAC and TS but not positioned as in **I**, **II**, and **III**. Thus, the carboxylate groups of **VI**, NAC, and TS are in position to enter into electrostatic bonding with Arg11* and Arg28 at the active site. This explains the observed 100-fold increased binding of **VI**, as compared to the predominant

Chart 5

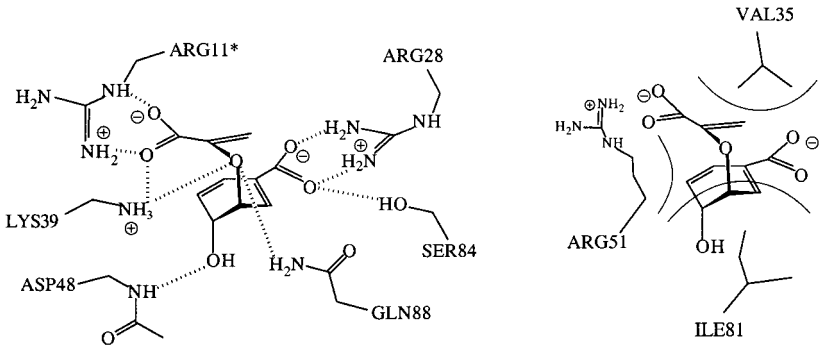

A. Electrostatic Interaction

B. Hydrophobic Interaction

Chart 6

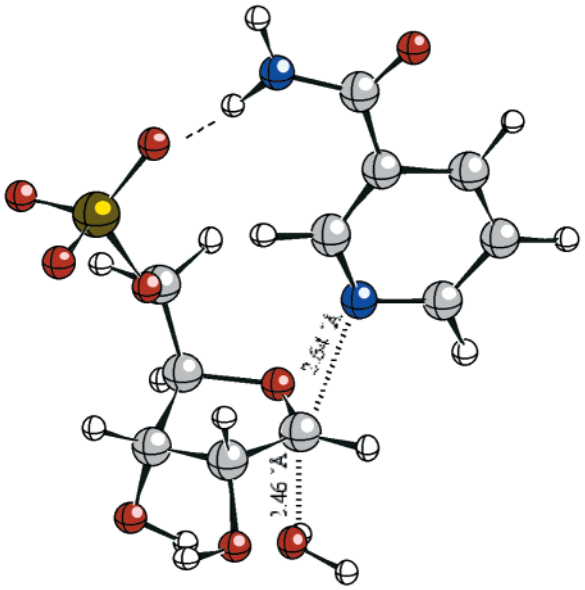

chorismate conformers (**I**, **II**, **III**).[38] **VI** is as much a ground-state "NAC analog" inhibitor as a TS analogue inhibitor.

Other enzymatic reactions which involve only electrostatic and hydrophobic interactions between E and TS may be found among reactions in which a first-order decomposition of a glycoside or a nucleoside involves an oxocarbenium-ion-like transition state. ADP-ribosylating toxins[4] are a well-studied group of enzymes. From multiple kinetic isotope effects,[39] the structure of the TS for the diphtheria-toxin-catalyzed hydrolysis of NAD^+ is known to be an exploded ribo-oxocarbenium ion in which the bond order to the leaving nicotinamide nitrogen is 0.02 and the bond order to the entering water oxygen is 0.03 (Chart 6). There is an X-ray structure of the E·NAD^+ complex of the complete ribosylating apparatus but not of the NAD^+ hydrolase portion. Employing the former, the latter was generated, and since the structure of the transition state is known, the E·TS structure can be generated. Scheme 1 and eq 2 can be investigated, since the TS structures for hydrolysis have been shown to be much the same in water[40] and in the enzyme. Since, $K_S/K_{TS} = 6000$ (ref 39), the transition-state binding hypothesis would have enzyme binding of the common TS exceed that for substrate binding by 6000-fold.

Ab initio calculations establish (i) the lowest-energy ground state of N-substituted and positively charged nicotinamides (such as NAD^+) has the carboxamide group in a cis configuration, with the carbonyl oxygen pointing in the direction of C2; and (ii) the most stable conformer of non-N-substituted neutral nicotinamide has the trans configuration, with the carbonyl oxygen pointing toward the C4 atom. The carboxamide group of enzyme-bound NAD^+ is trans, which means that strained substrate gives way to relaxed product, and since the TS is much advanced, the strain in the ground state is essentially relieved in the transition state. Ab initio calculations predict that this release of ground-state strain provides about 40% of the free energy of activation advantage of the enzymatic reaction, as compared to the solvolysis of NAD^+ in water.

From MD simulations of E·TS and the diphtheria toxin−NAD^+ complex, we find[41] the following features. Although the ribose 3′-OH is endo in the X-ray structure, there is a change during the MD simulation to 3′-exo in E·NAD^+ prior to formation of the E·TS in which the ribose 3′-OH is exo. This feature has been predicted from experimental KIE measurements in Schramm's laboratory.[39] Adjacent to the positively charged N1 of NAD^+ is negatively charged Glu148−CO_2^- (4.5 Å) and the negative oxygens of ribose C5−O−(PO_2^-)− (4.5 Å). On going from E·NAD^+ to E·TS, the nicotinamide ring has essentially departed as an almost neutral species, and the positive charge now resides principally on the oxygen and C1 of the appearing ribosyl oxocarbenium ion (Chart 6). The distances of Glu148−CO_2^- and the negative oxygens of ribose C5−O−(PO_2^-)− from the positive charge (now primarily on oxocarbenium ion C1 in the E·TS) are very much the same as in E·NAD^+. Face-to-face contact of the nicotinamide ring with the aromatic ring of Tyr65 and hydrogen bonding between the Gly22 peptide linkage and the nicotinamide carboxamide side chain remain essentially unchanged when E·NAD^+ approaches E·TS. The ribose 2′-OH is hydrogen-bonded to Glu148−CO_2^- ~20% of the time in E·NAD^+ and ~60% of the time in E·TS. In the E·NAD^+ complex, the side chain carbonyl of Asn45 is hydrogen-bonded to the ribose 2′-OH (12% of the time)

and 3′-OH (33% of the time). This hydrogen bonding was absent in E·TS. Thus, at the reaction center, electrostatic and hydrophobic interactions in E·S and E·TS are much the same (Stereoview of E·TS structure around the bond breaking site in Chart 7). Comparing the restriction of movements of the entire NAD^+ and TS entities, it is found that up to 1 ns, NAD^+ and TS have comparable average thermal positional flutuations when enzyme-bound.

It is known that ionization of the 2′-OH of the nicotinamide-bound ribose brings about a 10 000-fold increase in the rate of hydrolysis of NAD^+ in water.[42] Thus, ionization of the ribose 2′-OH increases the rate of hydrolysis more than does the enzymatic reaction. One would suppose that the mechanism of the enzymatic reaction would include this feature. The partial negative charge imposed on the 2′ oxygen when hydrogen-bonded to Glu148$-CO_2^-$ would be expected to be of some importance in enzymatic catalysis. Mutagenesis experiments, however, have shown that glutamine or aspartate residues replace Glu148 without loss of hydrolytic activity.[43] In summary, 40% of the acceleration of NAD^+ hydrolysis by the hydrolase enzyme arises from release of ground-state strain. The factors responsible for the remainder of the acceleration remain unidentified. Some portion of this could be due to preferential TS binding.

A 1.5-Å resolution X-ray structure of an ADP ribosyltransferase (VIP2), which is a bacterial vegetative insecticidal protein (VIP), has been recently reported.[44] The active site is much the same as that of diphtheria toxin. The structure of the active site of the VIP2·NAD^+ complex (2.7 Å) has been interpreted to indicate that formation of the ribosyl oxocarbenium ion does not involve TS stabilization.

7. How Formation of NAC Structures Lower $\Delta G^{\ddagger}$ Compared to $\Delta G^{\ddagger}$ for the Noncatalyzed Reaction

The energies of E·S conformers are predetermined by the shape of the active site, the distribution of its charges, and dipolar and hydrophobic interactions with the substrate. On the basis of these energies, the populations of the various conformers are determined by a Boltzmann distribution (Figure 2).[25] If NAC populations are as low as 1 mol % of total E·S conformers, the free energy content of the NAC is no more than ~2 kcal/mol above that of the average E·S conformer. In the few extended MD simulations of total E·S that have been carried out, NAC conformers represent between 1 and 70 mol % of total conformers.[36,45−51] The reaction trajectories of an enzymatic and a nonenzymatic reaction are compared in Figure 3. According to Figure 3, the kinetic advantage of the enzymatic reaction compared to the nonenzymatic reaction is the ease of formation of NAC structures and the favorable free-energy difference between NAC and TS. In other words, the enzyme increases the mole percent of conformers that are NACs. NACs are the turnstiles through which substrate must pass to become the lowest-energy TS.

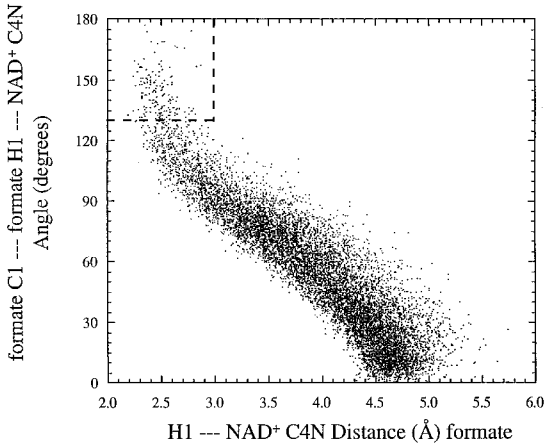

FIGURE 2. Plot of the vertical angles of approach between formate and nicotinamide [(NAD^+)C4····(formate)H1····(formate)C1] vs distance between NAD^+ C4 and (formate)H1. The plot contains ~9500 conformers at the active site of formate dehydrogenase sampled by MD simulations. NACs are found in the box in the left-hand corner.

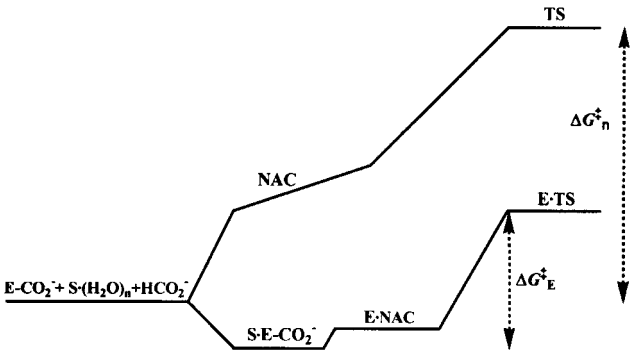

FIGURE 3. Cartoon of the coordinates for formation of transition states (TS) in the reactions involving (i) an enzymatic reaction in which active site Asp$-CO_2^-$ makes a covalent bond with substrate, and (ii) the nonenzymatic analogy in which formate attacks substrate. The common ground state is indicated by {E$-CO_2^-$ + S·$(H_2O)_n$ + HCO_2^-}. The formation of the enzyme−substrate complex (S·E$-CO_2^-$) involves desolvation of S·$(H_2O)_n$ and $K_S = 5 \times 10^{-5}$. Ground state MD simulation studies indicate that only ~1% of the (S·E$-CO_2-$) conformers are near-attack conformers (abbreviated E·NAC). Thus, the E·NAC conformers are ~2 kcal/mol in free energy above the ground state shared by 99% of S·E$-CO_2^-$ conformers. The corresponding enzyme transition state structure (abbreviated E·TS) has been taken as being 8 kcal/mol above E·NAC. In the uncatalyzed reaction, the HCO_2^- and S reactants have to find each other as near-attack conformers, which involves desolvation of the nucleophilic carboxylate group. NACs in noncatalyzed reactions do not represent detectable minimums along the reaction trajectory. The transition state is assumed to be 13 kcal/mol above NAC in the nonenzymatic reaction. The difference in the free energy of activation ($\Delta G_E^{\ddagger}$) for nonenzymatic and enzymatic reactions is 11 kcal/mol; however, if one compares the free energy differences in going from NAC to TS, one finds the enzymatic reaction favored by but 5 kcal/mol. The figure is a cartoon. Only the mole fractions of enzyme·substrate complexes that are in a NAC are presently calculated. Calculations of mole fractions of reactants existing as NACs in bimolecular reactions in water have not been carried out; however, the mole fractions of NAC conformation in reactions of two species in an intramolecular reaction in water have been calculated (20).

The importance of the resemblance of the NAC structure to the most stable TS structure can be shown by

Chart 7

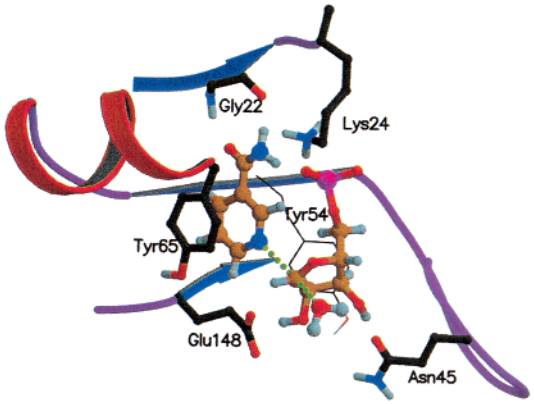

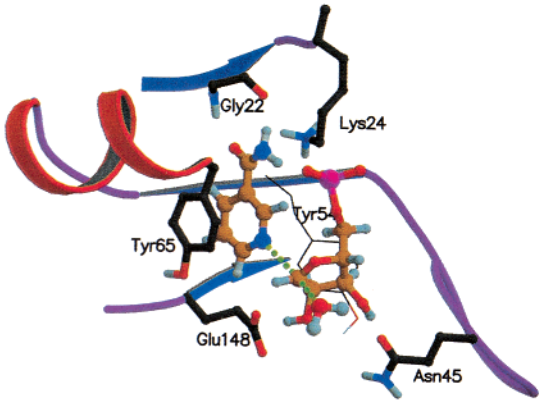

Chart 8

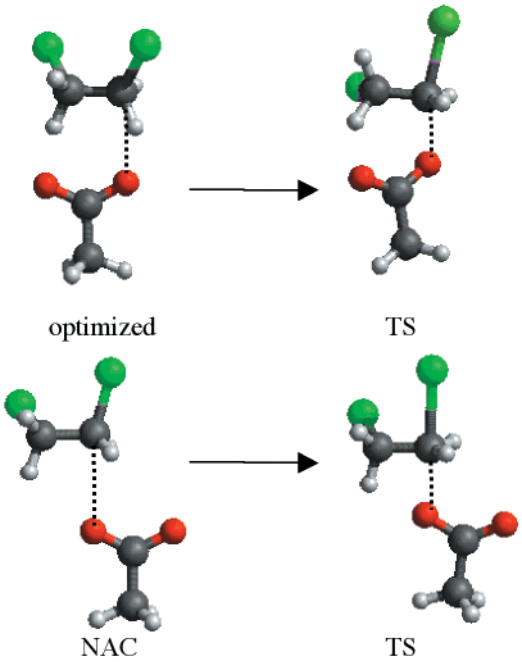

Chart 9

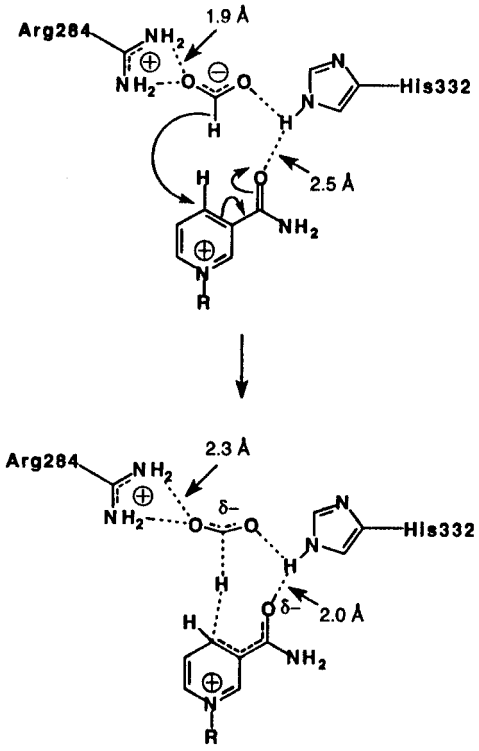

comparing the activation energies when starting with the most stable ab initio optimized ground-state structure and when starting with the NAC structure of the enzymatic reaction. Replacement of the most stable ground-state conformer by a NAC from the catechol *O*-methyltransferase MD simulation decreases the activation barrier for the S_N2 displacement of the sulfonium methyl group by 18 kcal/mol[52,53]. For the *Xanthobacter autotrophicus* haloalkane dehalogenase reaction, replacement of the optimized ground-state structure by NAC lowers the activation energy for the S_N2 displacement of Cl^- by Asp124–CO_2^- by 9 kcal/mol (Chart 8)[54] The NAC structure in the E·S complex of dihydrofolate reductase has the substrate and cofactor in a conformation that resembles an *exo*-TS, rather than an endo conformation that is energetically favored in the gas phase.[55] Like results have been reported with the Rubisco enzyme.[56]From the MD simulations of E·NAC and E·TS, we can observe the active site structures around the ground-state NAC and the TS. If the overall electrostatic, dipolar, and hydrophobic interactions are closely similar, then the TS is not bound significantly tighter than the ground-state NAC. For example,[47] in the formate dehydrogenase reaction, there are 11 electrostatic interactions between substrate and nicotinamide moieties in both NAC and TS. The overall stabilities of the electrostatic interactions are comparable because of compensating changes in the distances of two electrostatic interactions (Chart 9). Since electrostatic interactions with the E·NAC and E·TS of catechol *O*-methyltransferase are similar,[52,53] the rate enhancement[57] of 10^{16} cannot be ascribed to TS binding by enzyme. Much the same is true for the other enzymatic reactions that we have examined.[20,37,47,52,54,56,58]

8. Conclusions

The transition state in an enzymatic reaction is reached through ground-state conformers that closely resemble the transition state (near-attack conformers or NACs).[12,20] The

mole percentage of E·S conformers present as E·NACs amounts to ≥1% (Figure 3). Thus, the free energy content of the enzyme bound NAC is no more than 2 kcal/mol greater than that of the average enzyme-bound conformers of S. In gas-phase calculations, it can be shown that the activation energy for NAC → TS is *much* less than the activation energy required for conversion of the optimized most stable nonenzymatic ground-state conformers → TS. The electrostatic interactions that are complementary between the active site and NAC may also be complementary to TS. Retaining complementarity when the polarity of the TS is much different from the NAC comes about by changes in the distances of electrostatic interactions that reflect changes in polarization.

The belief that enzymatic reactions owe their facility to TS binding or to an increase in $\Delta S^{\ddagger}$ requires modification.

The author expresses gratitude to the National Institutes of Health (5R37DK09171-36) and the National Science Foundation (MCB 9727937) for support and to Dr. Paula Y. Bruice, Dr. Kalju Kahn, and Ms. Sun Hur for conversations and advice.

References

(1) Pauling, L. Molecular Architecture and Biological Reactions. *Chem. Eng. News* **1946**, *24*, 1375−1377.
(2) Pauling, L. Nature of Forces Between Large Molecules of Biological Interest. *Nature* **1948**, *161*, 707−709.
(3) Lolis, E.; Petsko, G. A. Transition-State Analogues in Protein Crystallography: Probes of the Structural Source of Enzyme Catalysis. *Annu. Rev. Biochem.* **1990**, *59*, 597−630.
(4) Schramm, V. L. Enzymatic Transition States and Transition State Analogue Design. *Annu. Rev. Biochem.* **1998**, *67*, 693−720.
(5) Bruice, T. C.; Schmir, G. L. The catalysis of the hydrolysis of *p*-nitrophenyl acetate by imiazole and its derivatives. *Arch. Biochem. Biophys.* **1956**, *63*, 484−486.
(6) Bruice, T. C.; Schmir, G. L. The catalysis of hydrolysis of phenyl acetates by imidazole. *J. Am. Chem. Soc.* **1957**, *79*, 1663−1667.
(7) Bender, M. L.; Turnquist, B. W. General basic catalysis of ester hydrolysis and its relationship to enzymatic hydrolysis. *J. Am. Chem. Soc.* **1957**, *79*, 1056−1662.
(8) *Organic Reaction Mechanisms 1965*; Capon, B., Perkins, M. J., Rees C. W., Eds.; Interscience: London, 1965.
(9) Bruice, T. C.; Benkovic, S. J. *Bioorganic Mechanisms*; Benjamin: New York, 1966; Vol. 1, Chapter 1.
(10) Kirby, A. J. Effective molarities for intramolecular reactions. *Adv. Phys. Org. Chem.* **1980**, *17*, 183−278.
(11) Fife, T. H.; Chauffe, L. General base and general acid-catalyzed intramolecular aminolysis of esters. Cyclization of esters of 2-aminomethylbenzoic acid to phthalimidine. *J. Org. Chem.* **2000**, 65, 3579−3586
(12) (a) Bruice, T. C.; Pandit, U. K. Intramolecular models depicting the kinetic importance of "fit" in enzyme catalysis. *Proc. Natl. Acad. Sci., U.S.A.* **1960**, *46*, 402−404. (b) Bruice, T. C.; Pandit, U. K. The effect of geminal substitution ring size and rotamer distribution on the intramolecular nucleophilic catalysis of the hydrolysis of monophenyl esters of dibasic acids and the solvolysis of the intermediate anhydrides. *J. Am. Chem. Soc.* **1960**, *82,* 5858−5865.
(13) Page, M. L. and Jencks, W. P. Rate accelerations in enzymatic and intramolecular reactions and the chelate effect. *Proc. Natl. Acad. Sci U.S.A.* **1971**, *68*, 1678−1683.
(14) Jencks, W. P. Binding energy, specificity, and enzyme catalysis: The Circe Effect. *Adv. Enymol.* **1975**, *43*, 223.
(15) Wolfenden, R.; Snider, M.; Ridgway, C.; Miller, B. The temperature dependence of enzyme rate enhancements. *J. Am. Chem. Soc.* **1999**, *121*, 7419−7420.
(16) (a) Chen, J.; Deng, Q.; Wang, R.; Houk, K. N.; Hilvert, D. A theoretical study of Diels−Alder catalysis by antibody 1E9. *Chembioche.* **2001**, *1*, 255−261. (b) Murphy, K. P.; Xie, D.; Thompson, K. S.; Amzel, L. M.; Freire, E. Entropy in Biological Binding Processes: Estimation of translational entropy loss. *Proteins* **1994**, *18*, 63−67.
(17) Kast, P.; Asif-Ullah, M.; Hilvert, D. Is chorismate mutase a prototypic entropy trap? Activation parameters for the B. *subtilis* enzyme. *Tett. Lett.* **1996**, *37*, 2691−2694.
(18) Srinivasan, R.; Fisher, H. F. Comparison of the energetics of the uncatalyzed and glutamate dehydrogenase catalyzed α-imino acid−α-amino acid interconversion. *Biochemistry* **1985**, *24*, 5356−5360.
(19) Jardetzky, O.; Lefevre, J. F. Protein dynamicas. *FEBS Lett.* **1994**, *338*, 246−250.
(20) Bruice, T C.; Lightstone, F. C. Ground-state and transition-state contributions to the rates of intramolecular and enzymatic reactions. *Acc. Chem. Res.* **1999**, *32*, 127−136.
(21) Lightstone, F. C.; Bruice, T. C. Separation of ground-state and transition state effects in intramolecular and enzymatic reactions. 2. *J. Am. Chem. Soc.* **1997**, *119*, 9103−9113.
(22) Villa, J.; Strajbl, M.; Glennon, T. M.; Sham, Y. Y.; Chu, Z. T.; Warshel, A. How important are entropic contributions to enzyme catalysis? *Proc. Natl Acad. Sci U.S.A.* **2000**, *97*, 11899−11904.
(23) (a) Saunders: M. Stochastic exploration of molecular mechanics energy surfaces. Hunting for the global minimum. *J. Am. Chem. Soc.* **1987**, *109*, 3150−3152. (b) Saunders: M. Stochastic search for the conformations of bicyclic hydrocarbons. *J. Comput. Chem.* **1989**, *10*, 203−208.
(24) Allinger, N. L.; Zhu, Z. Q. S.; Chen, K. Molecular mechanics (MM3) studies of carboxylic acids and esters. *J. Am. Chem. Soc.* **1992**, *114*, 6120−6133.
(25) Lightstone, F. C.; Bruice, T. C. Separation of ground state and transition state effects in intramolecular and enzymatic reactions. Part 1. *J. Am. Chem. Soc.* **1996**, *118*, 2595−2605.
(26) (a) Scheiner, S.; Lipscomb, W. N.; Kleier, D. A. Molecular orbital studies of enzyme activity. 2. Nucleophilic attack on carbonyl systems with comments on orbital steering. *J. Am. Chem. Soc.* **1976**, *98*, 4770−4777. (b) Kahn, K. Master's Thesis, University of Tartu, 1994, Chapter 2.
(27) Bruice, T. C.; Kahn, K. Computational Enzymology. *Curr. Opin. Chem. Biol.* **2000**, *4*, 540−544.
(28) Kollman, P. A.; Kuhn, B.; Donini, O.; Perakyla, M.; Stanton, R.; Bakowies, D. Elucidating the nature of enzyme catalysis utilizing a new twist on an old methodology: QM-free energy calculations on chemical reactions in enzymes and in aqueous solution. *Acc. Chem. Res.* **2001**, *34*, 72−79
(29) Bash, P. A.; Ho, L. L.; Mackerell, A. D.; Levine, D.; Hallstrom, P. Progress toward chemical accuracy in the computer simulation of condensed phase reactions. *Proc. Natl. Acad. Sci. U.S.A.* **1996**, *93*, 3698−3703
(30) Stanton, R. V.; Perakyla, M.; Bakowies, D.; Kollman, P. Combined ab initio and free energy calculations to study reactions in enzyme and solution: Amide hydrolysis in trypsin and aqueous solution. *J. Am. Chem. Soc.* **1998**, *120*, 3448−3457.
(31) Snider, M. J.; Gaunitz, S.; Ridgway, C.; Short, S. S.; Wolfenden. R. Temperature Effects on the Catalytic Efficiency, Rate Enhancement, and Transition State Affinity of Cytidine Deaminase, and the Thermodynamic Consequences for Catalysis of Removing a Substrate "Anchor". *Biochemistry* **2000**, *39*, 9746−9753.
(32) Bruice, T. C.; Benkovic, S. J. Chemical Basis for Enzyme Catalysis. *Biochemistry* **2000**, *39*, 6267−6274.
(33) Ganem, B. Chorismate Mutase. *Angew. Chem., Int. Ed. Engl.* **1996**, *35*, 937−945.
(34) Carlson, H. A.; Jorgensen, W. L. Monte Carlo Investigations of Solvent Effects on the chorismate to prephenate rearrangement. *J. Am. Chem. Soc.* **1996**, *118*, 8475−8484
(35) (a) Marti, S.; Andres, J.; Moliner. V.; Silla, E.; Tunon, I.; Bertran, J. A. QM/MM study of the conformational equilibria in the chorismate mutase active site. The role of the enzymatic deformation energy contribution. *J. Phys. Chem. B* **2000**, *140*, 11308−11313. (b) Marti, S.; Andres, J.; Moliner, V.; Silla, E.; Tunoon, I & Bertran, J. Transition structure selectivity in enzyme catalysis; a QM/MM study of chorismate mutase. *Theor. Chem. Acc.* **2000**, *105*, 207−212.
(36) Khanijin, N. A.; Snyder, J. P.; Menger, F. M. Mechanism of Chorismate Mutase: Contribution of Conformational Restriction to Catalysis in the Claisen Rearrangement. *J. Am. Chem. Soc.* **1999**, *121*, 11831−11846.
(37) Hur, S.; Bruice, T. C. The mechanism of catalysis of the chorismate to prephenate reaction in the E. coli mutase enzyme. *Proc. Natl. Acad. Sci. U.S.A.* **2002**, In Press.
(38) Bartlett, P. A.; Nakagawa, Y.; Johnson, C. R.; Reich, S. H.; Luis, A. Chorismate Mutase Inhibitors: Synthesis and Evaluation of Some Potential Transition-State Analogues. *J. Org. Chem.* **1988**, *53*, 3195−3210
(39) Berti, P. J.; Blanke, S. R.; Schramm, V. L. Transition state structure for the hydrolysis of NAD^+ catalyzed by diphtheria toxin. *J. Am. Chem. Soc.* **1997**, *119*, 12079−12088.

(40) Parkin, D. W.; Leung, H. B.; Schramm, V. L. Synthesis of nucleotides with specific radio labels in riboside. Primary carbon-14 and secondary tritium kinetic isotope effects on acid-catalyzed glycoside bond hydrolysis of AMP, dAMP, and inosine. *J. Biol. Chem.* **1984**, *256*, 9411−9417.
(41) Kahn, K.; Bruice, T. C. Diphtheria toxin catalyzed hydrolysis of NAD^+: Molecular dynamics study of enzyme bound substrate, transition state, and inhibitor. *J. Am. Chem. Soc.* **2001**, *123*, 11960−11969.
(42) Johnson, R. W.; Marschner, T. M.; Oppenheimer, N. Pyridine nucleotide chemistry. A new mechanism for the hydroxide-catalyzed hydrolysis of the nicotinamide-glycosyl bond. *J. Am. Chem. Soc.* **1988**, *110*. 2257−2263.
(43) (a) Wilson, B. A.: Reich, K. A.; Weinster, B. R..; Collier, R. J. Active-site mutations of diphtheria toxin: Effects of replacing glutamic acid-1438 with aspartic acid, glutamine, or serine. *Biochemistry* **1990**, *29*, 8643−8651. (b) Wilson, B. A.: Blanke, S. R.; Reich, K. A.; Collier, R. J. Active site mutations on diphtheria toxin. Tryptophan 50 is a major determinant of NAD affinity. *J. Biol. Chem*. **1994**, *269*, 23296−23301
(44) Han, S.; Craig, J. A.; Putnam, C. D.; Caroz, N. B.*;* Tainer, J. A. Evolution and mechanism from structures of an ADP-ribosylating toxin and NAD^+ complex. *Nat. Struct. Biol. Lett.* **1999**, *6*, 932−936.
(45) Lau, E. Bruice, T. C. Importance of correlated motions in forming highly reactive near attack conformations in catechol *O*-methyltransferase. *J. Am. Chem. Soc.* **1998**, 120, 12387−12394.
(46) Lau, E. Bruice, T. C. Active site dynamics of the *Hha*I methyltransferase: Insights from computer simulation. *J. Mol. Biol.* **1999**, *293*, 9−18.
(47) Torres, R.; Schiøtt, B.; Bruice, T. C. Molecular dynamic simulations of ground and transition states for the hydride transfer from formate to NAD^+ in formate dehydrogenase. *J. Am. Chem. Soc.* **1999**, *121*, 8164−8173.
(48) Radkiewicz, J. L.; Brooks, C. L. Protein dynamics in enzymatic catalysis: Exploration of dihydrofolate reductase. *J. Am. Chem. Soc.* **2000**, *122*, 225−231.
(49) Laitinen, T.; Rouvinen, J.; Perakyla, M. Inversion of the roles of the nucleophile and acid/base catalysis in the covalent binding of epoxalkyl xyloside inhibitor to the catalytic glutamates of endo-1,4-*b*-xylanase (XYNII): a molecular dynamics study. *Prot. Eng.* **2000**, *13*, 247−252
(50) Luo, J.; Bruice, T. C. A molecular dynamics study of an NAD^+ dependent alcohol dehydrogenase (HLADH): Structures at the active sites of HLADH·NAD^+·$PhCH_2OH$, HLADH·NAD^+·$PhCH_2O^-$, and HALDH·NADH·PhCHO. *J. Am. Chem. Soc.* **2001**, *123*, 11952−11959.
(51) Lightstone, F. C.; Zheng, Y.-J.; Bruice, T. C. Molecular dynamic simulations of ground and transition states for S_N2 displacement of Cl^- from 1,2-dichloroethane at the active site of *Xanthobacter autotrophicus* haloalkane dehalogenase. *J. Am. Chem. Soc.* **1998**, *120*, 5611−5621.
(52) Lau, E.; Bruice, T. C. Comparison of the dynamics for ground state and transition state structures in the active site of catechol *O*-methyltransferase. *J. Am. Chem. Soc.* **2000**, *122*, 7165−7171.
(53) Kahn, K.; Bruice, T. C. Transition state and ground-state structures and their interaction with the active site residues in catechol *O*-methyltransferase. *J. Am. Chem. Soc.* **2000**, *122*, 46−51.
(54) Lau, E.: Kahn, K.; Bash, P. A.; Bruice, T. C. Importance of reactant positioning in enzyme catalysis. A hybrid quantum mechanics/molecular mechanics study of a Haloalkane Dehalogenase. *Proc. Natl. Acad. Sci.* U.S.A. **2000**, *97*, 9937−9942.
(55) Castillo, R.; Andres, J.; Moliner, V. Catalytic mechanism of dihydrofolate reductase enzyme. A combination QM/MM characterization of TS structure for the hydride transfer step. *J. Am. Chem. Soc.* **1999**, *121*, 12140−12147.
(56) Moliner, V.; Andres, J.; Oliva, J.; Safont, V. S.; Tapia, O. Transition state structure invariance to model system size and calculation levels: A QM/MM study of the carboxylation step catalyzed by Rubisco. *Theor. Chem. Acc.* **1999**, *101*, 228−233.
(57) Mihel, I.; Knipe, J. O.; Coward, J. K.; Schowen, R. L. α-Deuterium isotope effects and transition-state structure in an intramolecular model system for methyl-transfer enzymes. *J. Am Chem. Soc.* **1979**, *101*, 4349−4351.
(58) Thoden, J. B.; Huang, X. Y.; Raushel, F. M.; & Holden, H. M. The small subunit of carbamoyl phosphate synthetase: Snapshots along the reaction pathway, *Biochemistry* **1999**, *38*, 16158−16166.

AR0001665